Transactions of the Materials Research Society of Japan Vol.28 35-38 (2003)

Layered Structure Analysis of Magnetic Multilayers by X-ray Scattering and TEM Methods

Tatsumi Hirano, Kazuhiro Ueda and Takao Imagawa*
Hitachi Research Lab., Hitachi, Ltd., 7-1-1, Omika-cho, Hitachi-shi, Ibaraki-ken 319-1292, Japan
Fax: 81-294-52-7606, e-mail: hirano@gm.hrl.hitachi.co.jp
Fax: 81-294-52-7606, e-mail: ueda@gm.hrl.hitachi.co.jp
* Hitachi Global Storage Technologies, 2880 Kozu, Odawara-shi, Kanagawa-ken 256-8510, Japan
Fax: 81-465-47-5387, e-mail: takao.imagawa@hgst.com

The giant magnetoresistive head, consisting of magnetic and noble metal multilayers, is a key device of hard disk drives. As head properties strongly depend on the layered structure, structural characterization is important for producing good devices. In this report, we review energy-filter TEM for elemental mapping in nm resolution, multi-wave x-ray reflectometry for accurate analysis of the layer thickness, and in-plane diffraction for analysis of grain size and random strain. We also discuss applications of these methods and provide a future prospect.
Key words: Giant magnetoresistance, structure analysis, EF-TEM, x-ray reflectivity, in-plane diffraction

1. INTRODUCTION

Giant magnetoresistive (GMR) spin valve heads have been investigated for high recording density hard disk drives (HDD), because of their high sensitivity in reading magnetic records[1]. Recently, many researchers have investigated perpendicular magnetic recording media[2] and advanced spin valve heads with magnetic tunnel junctions (MTJ) for developing advanced HDD[3]. The MTJ structures which consist of two ferro-magnetic layers separated by a thin (~1 nm) tunnel barrier hold substantial potential for application as computer memory (MRAM)[4]. The GMR structures similarly consist of two ferro-magnetic layers separated by a noble metal spacer of a few nm thickness. Their magnetic properties, such as the magnetoresistance and interlayer coupling between the two ferromagnetic layers, strongly depend on the thickness and the interface roughness of each layer.

Therefore, a precise structural characterization of the magnetic multilayers is important for producing good devices and for improving their magnetic properties. Items to be identified in the structural characterization are as follows: 1) device structure under several processes; 2) elemental mapping and chemical bond information at nm region; 3) layer thickness, interface roughness and density; 4) crystal structure, orientation, strain and grain size; and 5) magnetization distribution, magnetic coupling, magnetic domain size and magnetic dynamics.

In this report, a few analysis methods for the structural characterization as mentioned above are reviewed by way of examples in our work.

2. ENERGY-FILTER TEM (EF-TEM)

2.1 Outline of EF-TEM

Transmission electron microscopes (TEM) have been used to give high resolution characterizations of microstructures. Recently, elemental mappings and chemical bonding states could be analyzed by a TEM equipped with a energy filter[5,6].

Electrons which enter a sample interact with, and are scattered by, atoms in the sample. The transmitted electrons consist of both elastic and inelastic scattered electrons. The latter are scattered by atoms in the inner shells (core-loss electrons), losing a certain amount of energy. This energy loss is unique for a given element. Thus it is possible to do elemental mapping by measuring the transmitted electron image selected at an energy by the energy filter equipment.

2.2 Experimental

As a example of elemental mapping, the magnetic layered structure of a GMR head was observed. The elemental images were acquired using a TEM (Hitachi, HF-2000) with an energy filter (Gatan, imaging filter model 678). The layered structure of the GMR head was NiFe shield/ Al_2O_3 under-gap/ PtMn/ CoFe/ Ru/ CoFe/ Cu/ CoFe/ NiFe/ CoFe/ Cu/ CoFe/ Ru/ CoFe/ PtMn/ Ta/ Al_2O_3 upper-gap / NiFe shield. The TEM sample of the GMR head device for cross-sectional observation was prepared using both a focused ion beam (FIB) and a micro-sampling technique by which the specific region of several μm can be picked up and thinned to a thickness of several tens of nm[7].

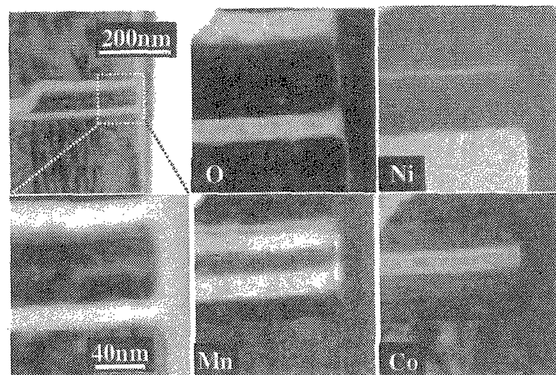

Fig.1 TEM images, O, Mn, Ni and Co core-loss images of the GMR head.

2.3 Results and Discussion

Fig.1 shows the TEM images, O, Mn, Ni and Co images. The brightness of these elemental images corresponds to the elemental concentration. The elemental images are in good agreement with the designed layered structure. In particular, six Co layers can be observed, i.e. the two thin (0.5 nm) CoFe layers and two CoFe layers separated by the thin (0.8 nm) Ru layer. Using these techniques, the layered structure of the head device can be analyzed precisely, e.g. not only lattice defects, stacking faults, dislocations and head shapes, but also elemental mappings and chemical bonding states.

2.4 Application of EF-TEM

The EF-TEM technique is indispensable for device development and failure analysis. The technique can be applied to observe element diffusions, changes of chemical bonding states with annealing, and fine processes.

3. MULTI-WAVE X-RAY REFLECTOMETRY[8]

3.1 Outline of MW-XRR

The x-ray reflectivity technique is a powerful tool for investigating layer thickness, electron density, and interface roughness[9]. However, in transition metal multilayers, such as CoFe/Cu/CoFe GMR multilayers, the difference in the refractive index between CoFe and Cu at Cu-Kα energy is too small to analyze precisely the layered structure, because of the lower intensity of specular x-rays reflected from CoFe/Cu interfaces. The refractive index is a strong energy-dependent variable and it rapidly changes near the absorption edge of the material. Fig.2 shows the x-ray intensity reflected from a Co/Cu interface as a function of x-ray wavelength. The reflected x-ray intensity is very strong at Cu-Kβ and Co-Kβ lines because of the anomalous-dispersion effect to enhance the x-rays reflected from the interface. The anomalous-dispersion effect is useful for more accurate analysis of the layered structure of transition metal multilayers[10-12]. Moreover, the analysis accuracy of the thickness and the interface roughness becomes higher by analyzing simultaneously the reflectivities measured at multi-x-ray wavelengths, because the problem of the local minimum in the least-squares method is avoided.

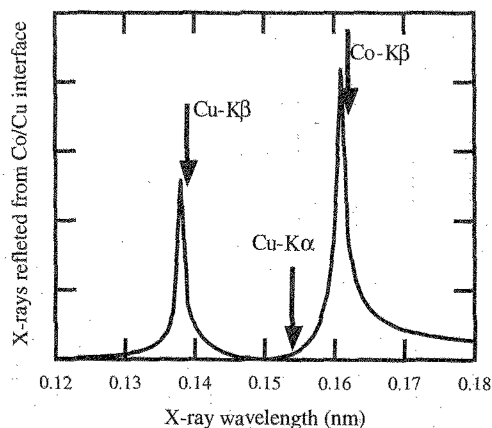

Fig.2 X-ray intensity reflected from Co/Cu interface as a function of x-ray wavelength.

3.2 Experimental

The layered structure of the GMR multilayer was Si sub./ Ta(5)/ NiFe(5)/ d-CoFe(1)/ Cu(2.3)/ u2-CoFe(2)/ Ru(t)/ u1-CoFe(1.5)/ CrMnPt(20)/ Ta(3). The numbers in parentheses are the nominal thickness in nm. The Ru thickness (t) was 0-0.8 nm. The reflectivities were measured at Co-Kβ, Cu-Kβ and Cu-Kα lines using an x-ray reflectometry instrument (Rigaku, SLX-1). They were measured using the θ-2θ scanning technique and simultaneously analyzed by the least-squares method, which uses the reflectivity formula and includes interfacial effects due to roughness and/or interdiffusion[13,14]. The values of refractive index (δ), thickness (t), and interface width (σ) for each layer were refined by minimizing χ^2;

$$\chi^2 = \sum_j \chi_j^2 = \sum_j \sum_i (\log I^i_{\exp} - \log I^i_{cal})^2_j, \quad (1)$$

where $I_{\exp}$ and I_{cal} were the experimental and calculated reflectivity intensities, respectively. j was the number of x-ray wavelengths, and i is the data point of reflectivity measured at each x-ray wavelength.

3.3 Results and Discussion

Fig.3 shows the experimental and calculated reflectivities measured at 3 x-ray wavelengths for the sample in the Ru layer of 0.4 nm thickness. The refined reflectivity curves closely match the experimental data. The designed Ru thickness dependence of the analyzed thickness in each layer is shown in Fig.4. The analyzed Ru thickness is in proportion to the designed one. The thickness of Cu and d-CoFe is constant for the designed Ru thickness. Similarly, the thickness of u1-CoFe and u2-CoFe is constant except for the designed Ru thickness of 0.2 nm. The total thickness of u1-CoFe and u2-CoFe is almost constant for the Ru thickness. The division of the total thickness to each u-CoFe thickness has some ambiguity. These results indicate that it is possible to analyze the magnetic multilayered structure in the thickness of sub-nm. In order to investigate the

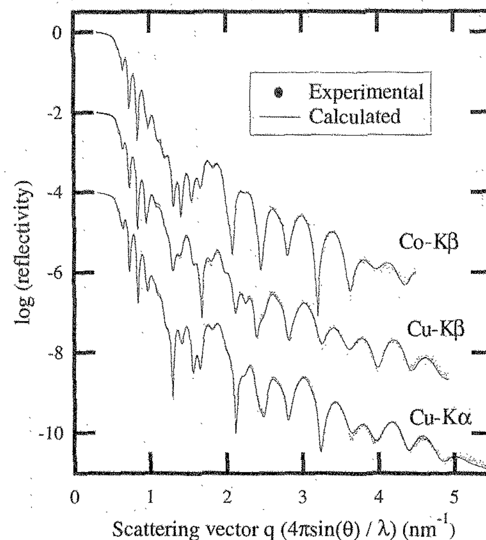

Fig.3 Experimental and calculated reflectivities measured at Co-Kβ, Cu-Kβ and Cu-Kα lines for the sample in the Ru layer of 0.4 nm thickness.

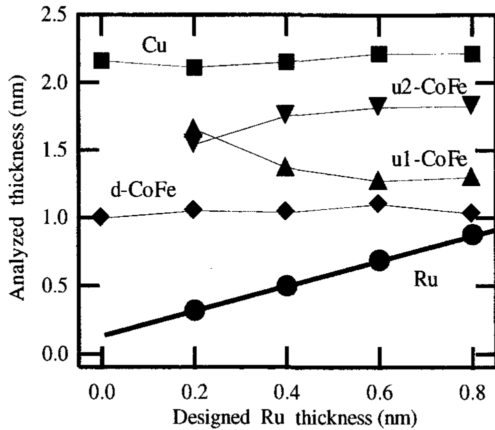

Fig.4 Designed Ru thickness dependence of analyzed thickness in each layer.

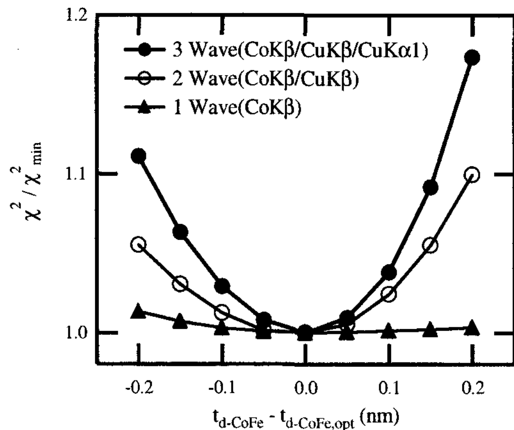

Fig.5 χ^2 distribution, ratio of χ^2 to the minimum value (χ^2_{min}), versus the offset value of the d-CoFe thickness from the optimum.

accuracy of the layered structure analysis using the MW-XRR method, d-CoFe thickness ($t_{d\text{-}CoFe}$) was kept fixed to a value offset from the optimum ($t_{d\text{-}CoFe,opt}$), and the other parameters were refined again. Fig.5 shows the χ^2 distribution, i.e., the ratio of χ^2 to the minimum value (χ^2_{min}) versus the offset value of the d-CoFe thickness from the optimum. As $|t_{d\text{-}CoFe} - t_{d\text{-}CoFe,opt}|$ is larger, χ^2/χ^2_{min} in the 3-wave method increases but χ^2/χ^2_{min} in the 1-wave method almost never changes. This indicates that $t_{d\text{-}CoFe}$ by the 3-wave method can be refined more accurately than that by 1- or 2-wave method.

3.4 Application of MW-XRR

Since the MW-XRR is a very accurate method to analyze multilayered structures, it can be applied to investigate the relationship between magnetic properties and layered structures, such as magnetoresistance versus thickness, density and interface roughness in each layer fabricated with an oxidation process.

4.IN-PLANE X-RAY DIFFRACTION (IP-XRD)[15,16]

4.1 Outline of IP-XRD

The IP-XRD technique is indispensable for investigating poly-crystal structure in the magnetic multilayer, such as orientations, strain and grain size. The sensitivity of the GMR head depends on the grain size and the strain of the magnetic free layer. Therefore, analysis of the size and strain is important for producing good GMR heads.

4.2 Experimental

The layers of the sample (A), PtMn(15)/ CoFe(2)/ Ru(1)/ FeOx/ CoFe(2)/ Cu(2)/ CoFe(2)/ Cu(1)/ AlOx/ Ta(1), were deposited on a glass substrate coated with an under-layer. The sample (B) structure having a RuOx layer is similar to sample (A) instead of a FeOx layer. The fcc(111) orientation of the layers of the samples is parallel to the normal of the glass substrate. The in-plane diffraction patterns of the samples were measured by a diffractometer at BL16XU in SPring-8 with an incident x-ray energy of 12.4 keV. To minimize the diffraction from the MnPt layer, the grazing incidence geometry was used with the incidence angle of 0.25 deg. The diffraction peaks were fitted by a Voigt function to obtain the peak width. The average crystallite size and the strain were analyzed using Hall's method, i.e. scattering vector dependence of the peak width[17].

4.3 Results and Discussion

The in-plane diffraction profiles of the fcc(220) and (440) peaks of the samples are shown in Fig. 6. The (440) peak FWHM of sample (A) is smaller than that of sample (B). The Hall's plot is shown in Fig. 7. The intercept point and the gradient mean the average

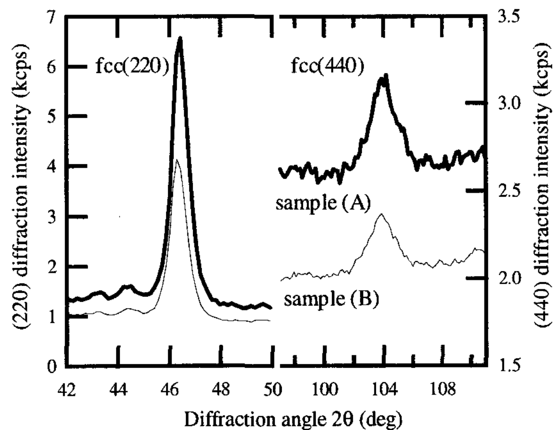

Fig.6 In-plane diffraction profiles of the fcc(220) and (440) peaks of the samples.

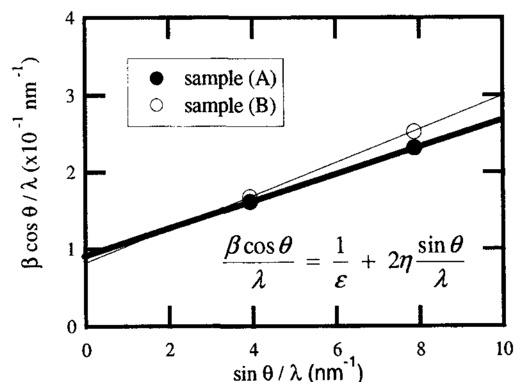

Fig.7 Hall's plot. β is peak's FWHM; ε, crystallite size; η, random strain; λ, x-ray wavelength.

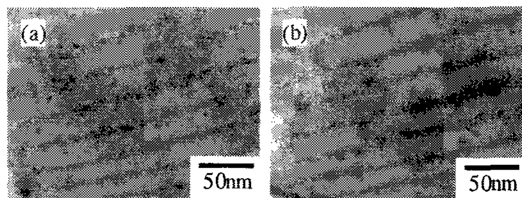

Fig.8 TEM images. (a) sample (A); (b) sample (B).

Table I Results of the crystallite size and the random strain of samples (A) and (B) using in-plane diffraction and TEM methods.

	TEM	In-plane diffraction	
	size(nm)	size(nm)	strain
sample (A)	7.3	8.5	0.009
sample (B)	12.5	10.5	0.014

crystallite size and the random strain, respectively. Both the crystallite size and the random strain of the magnetic layer in sample (A) were smaller than those of sample (B). Fig.8 shows the TEM images of the samples and it is clear that the grain size of sample (A) is smaller. The results obtained by IP-XRD and TEM show reasonable agreement (see Table I). Inserting the oxide layer in the GMR layer structure restricts the crystal growth from the substrate at the oxide layer. The good formation of the oxide layer such as FeOx will lead to small crystallite size and small random strain of the magnetic layer above the oxide layer. This causes the improvement of the soft magnetic property of sample (A).

4.4 Application of IP-XRD

IP-XRD is an indispensable method to analyze crystal structure in magnetic multilayers. It can be applied to investigate the relationship between the magnetic properties and the crystal structures such as grain size, strain, stacking fault, and so on.

5. FUTURE ANALYSIS

The full use of advanced analytical techniques is indispensable to investigate the structure of materials and devices and improve their properties. The performance of analytical instruments has been improved in resolution, sensitivity, accuracy and so on. The improved performance has been making it possible to observe reactions *in situ*. In the field of HDD, the following will be important: magnetic dynamics in the GHz region, contact phenomenon between head and media, local structure and dynamics of the magnetic moment, and so on.

Acknowledgments

We would like to express our thanks to S. Narishige and T. Kawabe of Hitachi Global Storage Technologies for useful discussions and their support. We would also like to thank K. Usami, N. Kobayashi and H. Momose of Hitachi Ltd. for useful discussions and their help and Y. Kozono, T. Suzuki, T. Aoyama, T. Miwa and T. Naitou of Hitachi Ltd. for their encouragement.

References

[1] B. Dieny, V. S. Speriosu, S. S. Parkin, B. A. Gurney, D. R. Wilhoit and D. Mauri, *Phys. Rev. Lett.*, **B43**, 1297-300 (1991).
[2] M. Futamoto, Y. Hirayama, Y. Honda, K. Itoh and K. Yoshida, *J. Magn. Soc. Jpn.*, **21**, 141 (1997).
[3] J. S. Moodera, and G. Mathon, *J. Magn. Magn. Mater.*, **200**, 248 (1999).
[4] S. S. P. Parkin, K. P. Roche, M. G. Samant, P. M. Rice, R. B. Beyers, R. E. Scheuerlein, E. J. O'Sulivan, S. L. Brown, J. Bucchigano, D. W. Abraham, Y. Lu, M. Roks, P. L. Trouilloud, R. A. Wanner and W. J. Gallagher, *J. Appl. Phys.*, **85**, 5828-33 (1999).
[5] K. Kimoto, T. Hirano, K. Usami and H. Hoshiya, *Jpn, J. Appl. Phys.*, **33**, L1642-44 (1994).
[6] T. Sekiguchi, K. Kimoto, T. Aoyama and Y. Mitsui, *Jpn, J. Appl. Phys.*, **37**, L694-96 (1998).
[7] T. Ohnishi, H. Koike, T. Ishitani, S. Tomimatsu, K. Umemura and T. Kamino, Proc. 25th Intern. Sympo. for Testing and Failure Analysis, 449-453 (1999).
[8] K. Usami, T. Hirano, N. Kobayashi, Y. Tajima and T. Imagawa, *J. Magn. Soc. Jpn.*, **24**, 551-54 (2000).
[9] T. C. Huang, J. -P. Nozieres, V. S. Speriosu, H. Lefakis and B. H. Gurney, *Appl. Phys. Lett.*, **60**, 1573-75 (1992).
[10] J. Bai, E. E. Fullerton and P. A. Montano, *Physica B*, **221**, 411-15 (1996).
[11] K. Usami, K. Ueda, T. Hirano, H. Hoshiya and S. Narishige, *J. Magn. Soc. Jpn.*, **21**, 441-44 (1997).
[12] T. Hirano, K. Usami, K. Ueda and H. Hoshiya, *J. Synchrotron Rad.*, **5**, 969-71 (1998).
[13] L. G. Parratt, *Phys. Rev.*, **95**, 359-69 (1954).
[14] L. Nevot, and P. Croce, *J. Rev. Phys. Appl.*, **15**, 761-79 (1980).
[15] K. Ueda, T. Hirano, M. Hasegawa and Y. Hirai, "SPring-8 User Experimental Report No.9", Japan Synchrotron Radiation Research Institute, 285 (2002).
[16] K. Hoshino, T. Imagawa, S. Shigematsu, K. Ueda and T. Hirano, *J. Magn. Soc. Jpn.*, **27**, 311-15 (2003).
[17] I. Nitta, "X-ray crystallography Vol.2", Maruzen, Tokyo (1962), p.618.

(Received July 31, 2003; Accepted August 21, 2003)